Strong-field magnetoresistance anisotropy in thin composite films with a periodic microstructure

David J. Bergman and Yakov M. Strelniker
School of Physics and Astronomy, Raymond and Beverly Sackler Faculty of Exact Sciences, Tel Aviv University, Tel Aviv 69978, Israel
(Received 2 December 1994)

The possibility of observing angular magnetotransport anisotropy in a thin conducting film with a periodic array of macroscopic inclusions is discussed. We consider a geometry in which the magnetic field and the volume-averaged current density are mutually perpendicular and both lie in the plane of the film and we study how the resistivity changes when they are rotated in this plane. We show that magnetotransport anisotropy, similar to what has recently been predicted to occur for infinite three-dimensional periodic composites, should appear even in the case of a thin film.

The strong-field magnetoresistance of a composite medium with a *periodic microstructure* was recently predicted by us to exhibit a strong dependence on the precise orientations of the external magnetic field $\mathbf{H}$ and the volume-averaged current density $\langle \mathbf{J} \rangle$, very similar to its behavior in certain metallic single crystals (see Fig. 14 in Ref. 1). This effect has yet to be verified experimentally. Unfortunately, measurements of magnetotransport in composite conductors are quite rare and until now were confined to disordered composite media:[2,3] periodic composite media are not commonplace. Although three-dimensional (3D) periodic *dielectric* composites are now used in order to achieve photonic band-gap environments,[4] 3D periodic *conducting* composites have not yet been fabricated, as far as we know. Also, in order to observe the effects predicted in Ref. 1, at least one component must have a large electron mobility in order to achieve a large value of the dimensionless magnetic field H, which is actually equal to the Hall-to-Ohmic resistivity ratio. It seems to us that the only system on which the necessary experiments could be carried out now is a thin film with a 2D periodic array of inhomogeneities. Such systems can be conveniently fabricated using the same microlithographic techniques that are used to fabricate arrays of quantum dots. We, therefore, extend the theory and the calculations, previously developed for 3D systems, to a discussion of magnetotransport in thin film composite media.

It is known that in the strictly two-dimensional case there is no magnetoresistance in composites (made of components that have no intrinsic magnetoresistance) when $\mathbf{H}$ is perpendicular to the system plane.[5] By contrast, a 3D composite with a regular array of *infinitely long cylinders* exhibits a strong magnetoresistance when the magnetic field $\mathbf{H}$ lies in the plane perpendicular to the cylinder axes.[1] This is due to the fact that the current distortions are in fact three dimensional, i.e., they have an appreciable component along the cylinder axes. (This component appears as a consequence of the Lorentz force or the Hall effect in the distorted current field.) We expect that, even in a composite of finite thickness, magnetoresistance will appear for the same reason and that it will have similar properties. An important question is then: how thick must the film be in order to exhibit a large anisotropic magnetoresistance when H is large? As a result of the work reported below, we conclude that for an array of insulating cylindrical inclusions of radius R in a free-electron-like film of thickness l, a large, anisotropic magnetoresistance appears as soon as $Hl \gtrsim R$. This conclusion is based upon analytic as well as numerical calculations.

In order to gain some intuitive insight about this problem, we first argue heuristically as follows: Consider a film with a 2D array of such cylindrical inclusions of finite length l (equal to the film thickness) and radius R. We take both $\mathbf{H}$ and $\langle \mathbf{J} \rangle$ to lie in the film plane (that is the y, z plane—a schematic picture of the film appears as part of Fig. 1) perpendicular to the cylinder axis. The main problem is how to deal with the boundary condition $J_x = 0$ at the film surfaces. Starting from $\nabla \cdot \mathbf{J} = 0$, we average over the film thickness to get

$$0 = \overline{\nabla \cdot \mathbf{J}} \equiv \frac{1}{l} \int dx \, (\nabla \cdot \mathbf{J}) = \frac{\partial}{\partial y} \overline{J_y} + \frac{\partial}{\partial z} \overline{J_z} + \frac{1}{l} [J_x]_{x=0}^{x=l}, \tag{1}$$

where the overline denotes averaging *over the film thickness only*, so that the averaged quantities still depend upon y and z. The last term vanishes because $J_x = 0$ at the surfaces; therefore, we are left with a vanishing 2D divergence of the 2D averaged current density $\mathbf{J}_2 \equiv \overline{J_y} \mathbf{e}_y + \overline{J_z} \mathbf{e}_z$, namely, $\nabla_2 \cdot \mathbf{J}_2 = 0$. Using the explicit form of the resistivity tensor $\hat{\rho}$ for the component materials with H directed along the z axis

$$\hat{\rho} = \rho_0(y,z) \begin{pmatrix} 1 & -H & 0 \\ H & 1 & 0 \\ 0 & 0 & 1 \end{pmatrix}, \tag{2}$$

we can express the electric field $\mathbf{E}$ in terms of the current density as $\mathbf{E} = \hat{\rho}\mathbf{J}$. We now apply a similar averaging procedure to the other 3D Maxwell equation, $\nabla \times \mathbf{E} = 0$, to get

$$0 = \overline{(\nabla \times \mathbf{E})_x} = \frac{\partial}{\partial y} (\rho_0 \overline{J_z}) - \frac{\partial}{\partial z} \left(H \rho_0 \overline{J_x} + \rho_0 \overline{J_y} \right) \tag{3}$$

for the average of its x component. This can be rewritten

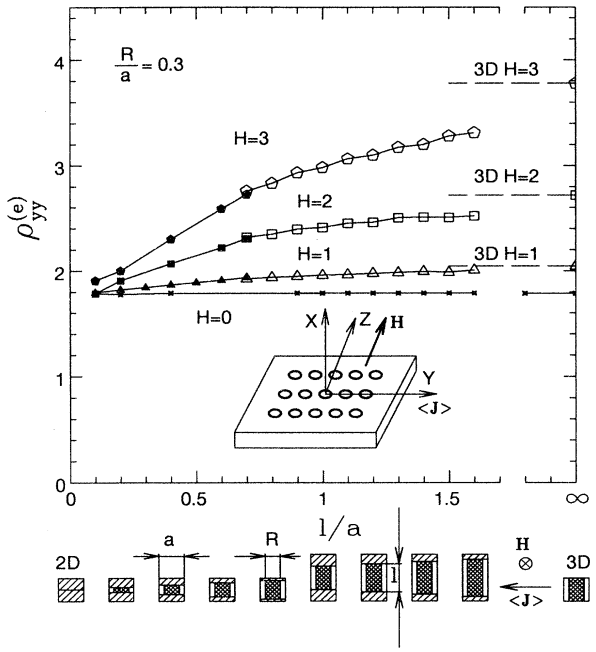

FIG. 1. Upper part: Magnetoresistance component $\rho_{yy}^{(e)}$ of a periodic composite film as function of the relative thickness l/a, where l is the absolute film thickness and a is the unit cell size of the square lattice. The volume-averaged current and the magnetic field are fixed along the coordinate axes in the film plane: $\mathbf{H} \parallel z$ and $\langle \mathbf{J} \rangle \parallel y$. The values used for $H \equiv |\mathbf{H}|$ are 0, 1, 2, 3. The inclusions (perfectly insulating cylinders with relative radius $R/a = 0.3$) form a square array and the host material is a free-electron-like metal with $\rho_0 = 1$. The solid symbols denote results obtained using the *cubic* 3D unit cell while the empty symbols denote results obtained using the *elongated tetragonal* 3D unit cell. These are explained below. The reciprocal lattice vectors used in these calculations ranged from -10 to 10 in each direction (see Ref. 1). Lower part: Schematic drawing of single unit cells of the 3D lattice with I-shaped insulating inclusions used in order to simulate films of *finite thickness* with insulating cylindrical inclusions. The magnetic field $\mathbf{H}$ and volume-averaged current density $\langle \mathbf{J} \rangle$ are always in the film plane, which is perpendicular to the cylinder axis. The hatched strips in the lower and upper parts of each unit cell represent the insulating layers. The cross-hatched area is the insulating cylinder of radius $R = 0.3a$ and length equal to the film thickness l. The size of the cubic unit cell is $a \times a \times a$. Such cells were used as long as $l \leq a$. In order to simulate films with $l \geq a$, we used elongated tetragonal unit cells where the length along the x axis is greater than a, specifically, we used a length equal to $2a$.

as

$$\nabla_2 \times (\rho_0 \mathbf{J_2}) = \frac{\partial}{\partial z} \left(\rho_0 H \overline{J_x}\right). \tag{4}$$

The right-hand side of this equation is estimated as follows: From $\nabla \cdot \mathbf{J} = 0$ we get $\partial J_x/\partial x = O\left(\partial J_y/\partial y\right) = O\left(\partial J_z/\partial z\right) \sim J_y/R \sim J_z/R$. Therefore, $J_x = O(lJ_y/R)$ and $\partial\left(\rho_0 H \overline{J_x}\right)/\partial z = O\left(\rho_0 H l J_y/R^2\right)$. This should be compared to the derivatives on the left-hand side of (4), which are all of order $\rho_0 J_y/R$. If $Hl/R \ll 1$, then the right-hand side of (4) is much smaller than those derivatives and we can write $\nabla_2 \times (\rho_0 \mathbf{J}_2) \approx 0$, which means that the magnetic field has *no effect* when $Hl \ll R$. We expect that the converse is also true, namely that as soon as $Hl \gtrsim R$, the magnetic field effects will be important and anisotropy will appear in the magnetoresistance of a quasi-2D periodic array.

We also performed numerical calculations of the bulk effective $\hat{\rho}_e$ for periodic thin film composites and the results corroborate this expectation. In order to avoid the computational complexity associated with the introduction of the $J_x = 0$ boundary condition at the film surfaces, our calculations were actually done on a 3D composite with a specific type of inclusion, namely a 3D simple cubic or tetragonal array of I-shaped insulators (with the "I" directed along the x axis—see the lower part of Fig. 1). This produces thin insulating layers parallel to the y, z plane, which split up the system into an unconnected family of parallel layers that represent the thin film. We solved this system using the same numerical scheme as in Refs. 1 and 6. That scheme is based upon a Fourier expansion of the periodic part of the electric potential $\phi(\mathbf{r})$, which is used to generate a power series expansion for the bulk effective conductivity tensor $\hat{\sigma}_e$ as function of the component conductivity tensors. The series, which is often divergent (especially for strong fields), is then summed by using Padé approximants.[6] Using this scheme it is possible to calculate $\hat{\sigma}_e$ and subsequently the bulk effective resistivity tensor $\hat{\rho}_e \equiv 1/\hat{\sigma}_e$. We applied this procedure to a free-electron-like metallic film inside which were embedded cylindrically shaped insulating inclusions arranged in a regular square array with their axes perpendicular to the film plane. The x axis was chosen to lie along those axes, perpendicular to the film plane, while the y, z axes were chosen to coincide with the axes of the square array.

In Fig. 1 we show the resistivity component $\rho_{yy}^{(e)}$ as function of the relative film thickness l/a (a is the lattice parameter) for different values of the dimensionless field parameter H when $\mathbf{H} \parallel z$ and $\langle \mathbf{J} \rangle \parallel y$. When $l/a = 0$ (see unit cell at the left-hand side of the lower part of Fig. 1) then the film is a strictly 2D system and $\rho_{yy}^{(e)}$ is independent of H. By contrast, when $l/a = \infty$ (see unit cell at the lower right-hand side part of Fig. 1) the film is a strictly 3D system and $\rho_{yy}^{(e)}$ has a strong H dependence for $H \gtrsim 1$, as found already in Ref. 1. For intermediate values of l/a, the H dependence of $\rho_{yy}^{(e)}$ is intermediate between those extremes. The different types of unit cell used in order to simulate films of different thicknesses are shown in the lower part of Fig. 1. When $H = 0$, the resistance is independent of the thickness. For $H > 0$, the resistance increases with both H and l. In agreement with the earlier considerations, the film surfaces are found to impede the development of current distortions and thus to reduce the effects of the magnetic field. With decreasing thickness l, the magnetoresistance $\rho_{yy}^{(e)}(\mathbf{H})$ decreases too, tending to $\rho_{yy}^{(e)}(0)$ when $l/a \to 0$. In the opposite limit $l/a \to \infty$, $\rho_{yy}^{(e)}(\mathbf{H})$ tends to the value found for a 3D composite with infinitely long cylindrical obstacles.

In practice the value of $\rho_{yy}^{(e)}(\mathbf{H})$ for films with $l = 2a$ is already not very different from the value at $l = \infty$.

We also studied the angular dependence of the transverse magnetoresistivity in the y, z plane, denoted by $\tilde{\rho}_{\perp}^{(e)}$ (this notation is the same as the one used in Ref. 1), as the direction of $\mathbf{H}$, and therefore also of $\langle \mathbf{J} \rangle$, was allowed to change in that plane (note that when $\mathbf{H} \parallel z$ and $\langle \mathbf{J} \rangle \parallel y$, $\tilde{\rho}_{\perp}^{(e)}$ is the same as $\rho_{yy}^{(e)}$).

In Fig. 2, we show results for $\tilde{\rho}_{\perp}^{(e)}$ in three samples with insulating cylindrical obstacles of different radii R. The distance from the origin in these plots gives the magnitude of $\tilde{\rho}_{\perp}^{(e)}(\mathbf{H})$ as function of the direction of $\mathbf{H}$ when its magnitude H is constant. Clearly, the magnetoresistance increases with both R and H. For large enough H, it develops a strong anisotropy, and the variations with the direction of $\mathbf{H}$ become more pronounced with *increasing* H but with *decreasing* R. The highest maxima are in the low order lattice directions equivalent to (001), then come those in the (011)-like directions, then (012), etc. For a given radius of the cylinders only a finite number of maxima appear, even if we keep increasing H, and the total number of maxima increases with decreasing radius. A

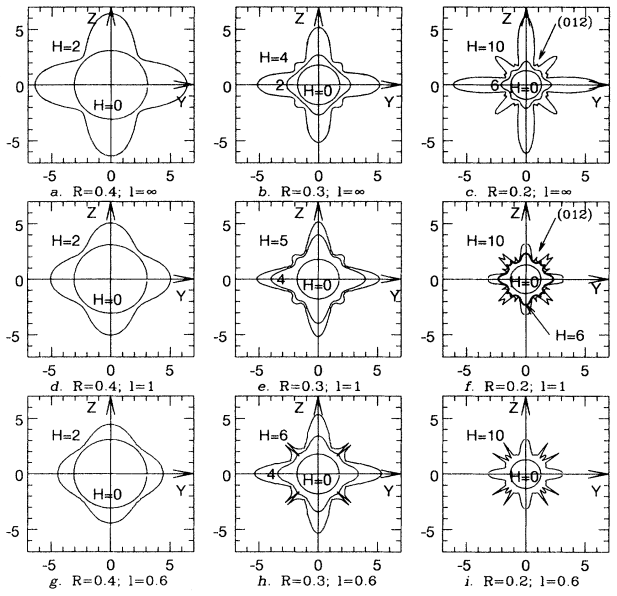

FIG. 2. Plots of the transverse magnetoresistance $\tilde{\rho}_{\perp}^{(e)}$ of three composite samples of insulating cylinders in a free-electron-like metallic host, for different film thicknesses l and cylinder radii R, arranged in a square array with unit cell size $a = 1$. The first line [(a), (b), (c)] exhibits control results corresponding to the 3D case of $l = \infty$. The second [(d), (e), (f)] and third [(g), (h), (i)] lines exhibit results for films with $l = 1.0$ and $l = 0.6$, respectively. The magnetic field $\mathbf{H}$ has a fixed magnitude $H \equiv |\mathbf{H}| \equiv \rho_{\mathrm{Hall}}/\rho_{\mathrm{Ohm}}$ and is rotated in the y, z plane. Note that the small maxima in the (012)-like directions in (c) and (f), one of which is marked by an arrow, are real, but that the jagged features that appear in some places in (f), (h), (i) are due to imperfect convergence of the Padé approximants and are spurious, as discussed in Ref. 1. The reciprocal lattice vectors used in these calculations ranged from -8 to 8 in each direction.

useful criterion for predicting when a maximum will appear in the $(0n1)$ direction seems to be $R < 2a/\sqrt{1+n^2}$: this was derived in Ref. 1 for a different transverse component of $\hat{\rho}_e$ and for a different type of array (i.e., for a simple cubic array of *spherical* obstacles or for a square array of infinitely long cylinders). This criterion appears to work quite well in the present case too, and it is in good *quantitative* agreement with the observed phenomenology (see Fig. 2), even though the simple arguments that were used to derive it are inapplicable here. We note that as R decreases, although the anisotropy of $\tilde{\rho}_{\perp}^{(e)}$ becomes more violent, higher values of H are needed in order to observe it. When l decreases, the anisotropy decreases in magnitude but its qualitative features remain unchanged. The jagged features that appear in Figs. 2(h), 2(f), and 2(i) near the (011)-like directions are spurious: They are due to imperfect convergence of the Padé approximants, as discussed in Ref. 1.

All results presented here were calculated for a composite with perfectly insulating inclusions. However, anisotropy is present even when the inclusions have a nonzero conductivity, as long as that is different from the surrounding conductivity and for sufficiently strong magnetic field.[1] It should also be mentioned that there are other types of composite film structures where similar phenomena should occur, for example, films with a periodically modulated surface thickness. In that case, the field $\mathbf{H}$ does not have to lie in the plane of the film: interesting anisotropies will appear even when $\mathbf{H}$ has a component along the perpendicular axis.[7]

We conclude with a discussion of some practical issues related to experimental testing of our predictions for thin films: It is possible to observe the anisotropy effect only when the magnetic field is strong enough, i.e., when $\rho_{\mathrm{Hall}} > \rho_{\mathrm{Ohm}}$, or equivalently $H \equiv \rho_{\mathrm{Hall}}/\rho_{\mathrm{Ohm}} = \omega_c \tau > 1$, in the host medium.[1] Since $\omega_c = e\mathcal{H}/m_e$ in SI units (m_e is the electron effective mass in kg, $\mathcal{H}$ is the magnetic field strength in tesla, e is the electronic charge in Coulomb), and since the relaxation time τ may be expressed in terms of the electric-field mobility of the electron $\mu = e\tau/m_e$, we can also rewrite this requirement as $H \equiv \mu\mathcal{H} > 1$. The mobility μ can have values within a very broad range, i.e., 10^{-7}–10 $\mathrm{m}^2/\mathrm{V\,sec}$, and depends on the materials used as well as on the temperature, since the electron-phonon interaction and the scattering by imperfections and impurities all affect the value of μ. It is thus possible to achieve the condition $H > 1$, even with a field as low as 1 T, by working at liquid helium temperatures and using either extremely pure (and therefore highly conducting) metals or else high mobility semiconductors.

The effect that we studied is entirely classical. Therefore, it is important to avoid quantum effects as much as possible, at least at the beginning, since those will only complicate the verification of predictions and interpretation of experiments. The electron mean free path should be small compared to all length scales associated with the inhomogeneity. Those include film thickness and inclusion sizes. Actually, we believe it will suffice if this restriction is satisfied by *either* the mean free path *or* the cyclotron radius, whichever is smaller; but, in order to

be on the safe side, we recommend that they both satisfy the restriction. Except for this restriction there is no absolute size parameter in this problem. However, there are relative lengths: the ratios R/a and l/a. For example, if $l = 100$ nm is a typical thickness of the film, then the unit cell size a should have approximately the same value. The cylinder radius should not be too small compared with a, e.g., $0.4a, 0.3a, 0.2a$ as in Fig. 2, since obstacles of smaller radius will result in smaller values of $\tilde{\rho}_{\perp}^{(e)}$ and faster oscillations of the angular profile. Consequently both high sensitivity and high angular resolution would be needed in order to detect those oscillations. Even the numerical calculations for samples with $R = 0.2a$ sometimes yield spurious results [see Figs. 2(f) and 2(i)].

In conclusion, the strong anisotropy of magnetoresistance that we have discovered in calculations on periodic composite conducting films, where the charge transport can be completely characterized by classical parameters like the resistivity tensor, should be observable in a properly designed experiment. Later, quantum corrections to this behavior may also prove worthwhile to pursue.

This research was supported in part by grants from the U.S.-Israel Binational Science Foundation and the Israel Academy of Sciences and Humanities.

[1] D. J. Bergman and Y. M. Strelniker, Phys. Rev. B **49**, 16 256 (1994).
[2] U. Dai, A. Palevski, and G. Deutscher, Phys. Rev. B **36**, 790 (1987).
[3] M. Rhode and H. Micklitz, Phys. Rev. B **36**, 7289 (1987).
[4] E. Yablonovich, T. J. Gmitter, and K. M. Leung, Phys. Rev. Lett. **67**, 2295 (1991).
[5] D. Stroud and D. J. Bergman, Phys. Rev. B **30**, 447 (1984).
[6] Y. M. Strelniker and D. J. Bergman, Phys. Rev. B **50**, 14 001 (1994).
[7] D. J. Bergman and Y. M. Strelniker (unpublished).